Golgi localization and phosphorylation of oxysterol binding protein in Niemann-Pick C and U18666A-treated cells

Abbas Mohammadi,[1] Ryan J. Perry, Margo K. Storey,[2] Harold W. Cook, David M. Byers, and Neale D. Ridgway[3]

Department of Pediatrics and Department of Biochemistry and Molecular Biology, Atlantic Research Centre, Rm 306, CRC Bldg., Dalhousie University, 5849 University Ave., Halifax, Nova Scotia, Canada B3H 4H7

Abstract **Oxysterol binding protein (OSBP) translocation between Golgi and vesicular/cytoplasmic compartments is affected by conditions that alter cholesterol and sphingomyelin homeostasis, indicating a role in lipid and sterol regulation in this organelle. In this study, we show that OSBP dissociation from the Golgi apparatus was inhibited when LDL cholesterol efflux from lysosomes was blocked in Niemann-Pick C (NPC) or U18666A {3-β-[2-(diethylamino)ethoxy]androst-5-en-17-one}-treated fibroblasts. Dissociation of OSBP from the Golgi apparatus in response to LDL was independent of de novo cholesterol biosynthesis. OSBP did not localize with filipin-stained lysosomal cholesterol, and the NPC defect did not alter OSBP expression or phosphorylation. However, OSBP in the Golgi apparatus was progressively dephosphorylated (as assessed by a molecular mass shift on SDS-PAGE) in U18666A-treated fibroblasts or Chinese hamster ovary cells as a result of combined inhibition of LDL cholesterol transport and de novo cholesterol synthesis. In vivo phosphopeptide mapping and mutagenesis of OSBP was used to identify the cholesterol-sensitive phosphorylation sites at serines 381, 384, and 387 that were responsible for the altered mobility on SDS-PAGE. NPC-1 protein-mediated release of LDL-derived cholesterol and de novo biosynthesis regulates OSBP localization and phosphorylation. This indicates that OSBP responds to or senses altered cellular sterol content and transport.**—Mohammadi, A., R. J. Perry, M. K. Storey, H. W. Cook, D. M. Byers, and N. D. Ridgway. **Golgi localization and phosphorylation of oxysterol binding protein in Niemann-Pick C and U18666A-treated cells. *J. Lipid Res.* 2001.** 42: **1062–1071.**

Supplementary key words Niemann-Pick type C • cholesterol • Golgi apparatus

Cholesterol synthesis in the endoplasmic reticulum (ER) and receptor-mediated uptake of LDL is subject to feedback suppression by cholesterol (1). The sites of cholesterol deposition in cells, as well as its concentration in membranes, are key determinants influencing regulation (2). The ER is the major site for cholesterol synthesis and harbors regulatory proteins and enzymes that are suppressed or activated by cholesterol, such as HMG-CoA reductase, sterol regulatory element binding protein (SREBP) precursors, and ACAT. The ER is also relatively poor in cholesterol compared with the plasma membrane (PM) (3), which contains 60–90% of cellular cholesterol (4). The bulk of cholesterol synthesized in the ER or delivered from lysosomes by the LDL receptor pathway is rapidly transported to the PM (5–8). When the capacity of the PM to absorb cholesterol has been exceeded, perhaps in response to sphingomyelin content (9, 10), cholesterol is transported to the ER where it down-regulates synthesis by transcriptional and post-transcriptional mechanisms. This explains the requirement for spatial separation of cholesterol from sterol-sensitive pathways in the ER. The proteins and mechanisms involved in cholesterol movement between these organelles are only now being understood.

Very few proteins have been identified that mediate or regulate intracellular cholesterol transport. One of these is the Niemann-Pick C protein (NPC1), a multitransmembrane-spanning protein that contains a cholesterol-'sensing' transmembrane domain also found in other cholesterol-sensitive proteins such as SREBP-cleavage activating protein (SCAP), HMG-CoA reductase, and the morphogen receptor PATCHED (11, 12). Mutations in the NPC1 gene lead to a progressive neurodegenerative disorder characterized by accumulation of cholesterol and sphingolipids in lysosomes or endosomes of affected tissues (12). The NPC1 protein mediates transport of cholesterol and sphingolipids from lysosomes or late endosomes to the PM or ER by a poorly defined vesicle trafficking pathway (13, 14). Another protein involved in

Abbreviations: ER, endoplasmic reticulum; FCS, fetal calf serum; NPC, Niemann-Pick C; OSBP, oxysterol binding protein; SREBP, sterol regulatory element binding protein; PM, plasma membrane; SRD, sterol regulation defective; U18666A, 3-b-[2-(diethylamino)ethoxy]androst-5-en-17-one.

[1] Present address: Biochemistry Dept., Afzalipoor Medical School, Shabab University, Kerman, Iran.

[2] Present address: National Jewish Medical and Research Center, Dept. of Medicine, 1400 Jackson St., Denver, CO 80206.

[3] To whom correspondence should be addressed.
e-mail: nridgway@is.dal.ca

sterol trafficking is caveolin, the major structural component of caveolar rafts. Caveolin is involved in delivery of newly synthesized cholesterol from the ER to PM, via the Golgi apparatus (15, 16).

We previously identified oxysterol binding protein (OSBP) as a potential cholesterol regulator or sensor in the Golgi apparatus. This was based on the observation that OSBP translocated to the Golgi apparatus in response to altered cholesterol trafficking, depletion of PM cholesterol (17, 18), and exogenous oxysterol ligands (19, 20). For example, OSBP localized to a vesicular/cytoplasmic compartment when CHO cells were replete with cholesterol (cultured in LDL), but moved to the Golgi in response to cholesterol depletion by treatment with cyclodextrin (17), delipidated serum (17, 18), or in cholesterol auxotrophic sterol regulation defective (SRD) 6 cells (18). U18666A, {3-β-[2-(diethylamino)ethoxy]androst-5-en-17-one}, a hydrophobic amine that prevents cholesterol efflux from lysosomes and phenocopies the NPC defect, prevented OSBP translocation from the Golgi in response to LDL in CHO cells (17). These results suggested that OSBP could be specifically responding to cholesterol transport to the Golgi apparatus, either from the lysosomes/endosomes, PM, or ER. The interaction of OSBP with elements of the Golgi apparatus in response to sterols is significant because this organelle has an established role in transport of de novo synthesized and LDL-derived cholesterol. The assembly of cholesterol/sphingolipid-enriched rafts and caveolae occurs in the Golgi (21, 22), and caveolin-containing rafts are involved in cholesterol transport from the ER to PM via the Golgi apparatus (15). Studies using brefeldin A have also shown that transport of LDL-derived cholesterol to the PM or ER involves the Golgi apparatus (6). Based on filipin binding experiments, the Golgi apparatus was shown to contain increasing amounts of cholesterol in a *cis* to *trans* gradient (23). This distribution of cholesterol is abnormal in NPC cells defective in efflux of cholesterol from lysosomes or endosomes (24). How cholesterol content and distribution in the Golgi apparatus is maintained is unknown. However, it is clear that cholesterol is required for the assembly of caveolae or rafts in the Golgi apparatus and subsequent sorting and delivery of proteins and lipids associated with these domains (21, 22, 25, 26).

In this study, we used NPC fibroblasts and drugs that alter cholesterol synthesis and transport to demonstrate that localization of OSBP to the Golgi apparatus is regulated by transport of LDL-derived cholesterol from a lysosomal or endosomal compartment. Localization of OSBP to the Golgi apparatus was not dependent on de novo synthesis. Using phosphopeptide mapping and site-directed mutagenesis, we also identified cholesterol-sensitive phosphorylation at serines 381, 384, and 387. These serines were dephosphorylated in response to inhibition by U18666A of LDL-cholesterol transport and de novo cholesterol synthesis. A model is proposed that summarizes how altered cholesterol homeostasis influences OSBP localization and phosphorylation, and indicates how OSBP functions as a downstream sensor of cholesterol transport in the Golgi apparatus.

MATERIALS AND METHODS

Cell culture

Normal (F8) and NPC (GM3123, 93.41, and 98.16) fibroblasts were maintained in MEM with 10% fetal calf serum (FCS). Cells were subcultured in MEM with 10% FCS in 60-mm dishes at a density that ensured 50–70% confluence on the day of experiments. Three days prior to the start of experiments, cells were switched into MEM with 5% delipidated FCS prepared by the Cab-O-Sil method (27). CHO-K1 cells were maintained and subcultured in DMEM with 5% FCS. Cells were switched to DMEM with 5% lipoprotein-deficient FCS 24 h prior to the start of experiments. Lipoprotein-deficient FCS was prepared by centrifugation at 1.21 g/ml, and human LDL was isolated from the 1.018–1.063 g/ml density interval of whole serum by centrifugation (28).

Site-directed mutagenesis

Site-directed mutagenesis of the rabbit OSBP cDNA in pCMV 2 was performed using the Gene Editor System (Promega) and confirmed by sequencing. The following oligonucleotides were used to mutagenize OSBP serine phosphorylation sites: S381A, CACAAACGTACTGGC**GC**CAACATCAGTGGA; S384A, GGCAGCACCATCG**CTG**GAGCCAGCAGT; S387A, ATCAGTG GAGCC**G**C CAGTGACATCAGC; S381E, AAACGTACTGGC **GAG**AACATCAGTGGAGCC; S384, 387E, CTGGCGAGAACATC **GAA**GGAGCC**GAA**AGTGACATCAGCCTTG.

Fluorescence microscopy

Cells were cultured on glass coverslips, fixed in 3% formaldehyde, and permeabilized in 0.05% Trition X-100 (20). Endogenous human OSBP was detected in permeabilized cells using affinity-purified polyclonal rabbit antibody 104 and FITC-labeled secondary antibody (17). Images of endogenous OSBP in fibroblasts were viewed with an Olympus microscope using a ×100 PlanApo objective and excitation/emission filters for FITC fluorescence. Cells were photographed using Kodak TMax 400 black and white film. For co-localization of cholesterol (visualized in cells by complexing with filipin) and OSBP, fibroblasts were viewed on an Axioplan II fluorescence microscope equipped with UV and FITC filters. Images of identical fields were captured using a SPOT cooled color digital camera and imported into Photoshop to create overlaid figures.

Immunoblotting, immunoprecipitation, and tryptic mapping

Fibroblasts were scraped from dishes into 10 mM phosphate (pH 7.4) and 150 mM NaCl (PBS) and collected by sedimentation at 5,000 rpm for 5 s in a microfuge. The cell pellet was disrupted by 20 passages through a 23-gauge needle in 10 mM HEPES (pH 7.4), 50 mM KCl, 5 mM DTT, 1 mM EDTA, and Complete protease cocktail (Boehringer Mannheim), and subjected to centrifugation at 200,000 *g* for 15 min. The membrane fraction (pellet) was solubilized in SDS sample buffer on ice for 5 min, separated on SDS-6% PAGE, and transferred to nitrocellulose. Filters were incubated with a C-terminal NPC1 anti-peptide antibody at a dilution of 1/3,000 and goat anti-rabbit horseradish peroxidase-conjugated secondary antibody (13). NPC1 was detected by the chemiluminescence method according to manufacturer's instructions (Amersham Pharmacia Biotech). Human OSBP was immunoblotted in soluble and particulate fractions of fibroblasts using a 1/10,000 dilution of polyclonal antibody 170. Antibody 170 was raised against a 100-amino acid C-terminal peptide from a 45-kDa OSBP-related protein (with >70% identity with OSBP) fused to glutathione *S*-transferase.

Total OSBP was extracted from CHO cell pellets with PBS containing Complete protease cocktail, 0.5% Triton X-100, 200 nM

okadaic acid, 2 mM EDTA, 2 mM EGTA, and 1 mM β-glycerophosphate. Cells were extracted on ice for 15 min and a detergent-soluble fraction was prepared by centrifugation in a microcentrifuge at 10,000 rpm for 10 min at 4°C. OSBP was detected by immunoblotting with antibody 170 as described above.

Wild-type and phosphorylation mutants of OSBP were transfected into CHO cells using Lipofectamine reagent (Gibco-BRL). Expression of transfected OSBP was determined by separating 0.5% Triton X-100 extracts of cells (as described above) by SDS-6% PAGE and immunoblotting with monoclonal 11H9 (20). Transfected CHO cells were labeled with $^{32}PO_4$ for the times indicated in figure legends, extracted with 0.5% Triton X-100, and immunoprecipitated with 11H9 as previously described (29). Immunoprecipitates were separated by SDS-6% PAGE and transferred to polyvinylidene diflouride (PVDF) membranes. Phosphorylated OSBP was excised from PVDF filters and subjected to tryptic digestion and two-dimensional phosphopeptide mapping (29).

RESULTS

Localization of OSBP in NPC fibroblasts

LDL-mediated dissociation of OSBP from the Golgi apparatus in CHO cells was blocked with U18666A, suggesting that OSBP translocation is linked to cholesterol transport from the lysosomes or late endosomes (17). However, in addition to disrupting cholesterol transport, U18666A also inhibits sterol synthesis (30) and may have other unknown pharmacological effects, thus making interpretation of results difficult. To resolve this question, we compared OSBP localization in U18666A and NPC fibroblasts that are defective in cholesterol transport from lysosomal or endosomal compartments due to defective NPC1 protein (11–14). Initially, normal fibroblasts were grown in medium with or without human LDL and U18666A for 18 h, and OSBP localization was assessed by indirect immunofluorescence. Similar to CHO cells, OSBP in fibroblasts grown in delipidated medium was concentrated in tubular fenestrated structures situated next to the nucleus (**Fig. 1A**). We confirmed that this was the Golgi apparatus, based on conversion to an ER-like pattern by brefeldin A treatment for 30 min, and co-localization with Golgi-specific FITC-lentil lectin (results not shown). In cells grown in LDL alone, there was still faint localization to the Golgi, but most OSBP was now situated throughout the cell in a diffuse punctate pattern (Fig. 1B). The inclusion of U18666A in medium containing LDL prevented the dissociation of OSBP from the Golgi apparatus (Fig. 1D). Cells grown in medium with delipidated serum plus U18666A had a staining pattern that was indistinguishable from cells grown in delipidated medium alone (Fig. 1C).

Having confirmed that OSBP localized to the Golgi apparatus in fibroblasts and that localization was affected by U18666A, we next examined localization of OSBP in two NPC fibroblast lines. OSBP was visualized by indirect immunofluorescence in NPC fibroblasts grown in the presence and absence of LDL for 18 h (**Fig. 2**). As expected, control fibroblasts displayed Golgi staining with OSBP antibodies in the absence of LDL, but not when cultured with LDL for 18 h. Two NPC cell lines displayed prominent Golgi localization of OSBP whether cultured in medium containing delipidated FCS for 3 days or medium containing LDL for 18 h. The NPC fibroblasts displayed a high level of autofluorescence around the Golgi apparatus caused by cholesterol-engorged lysosomes (see **Fig. 3**).

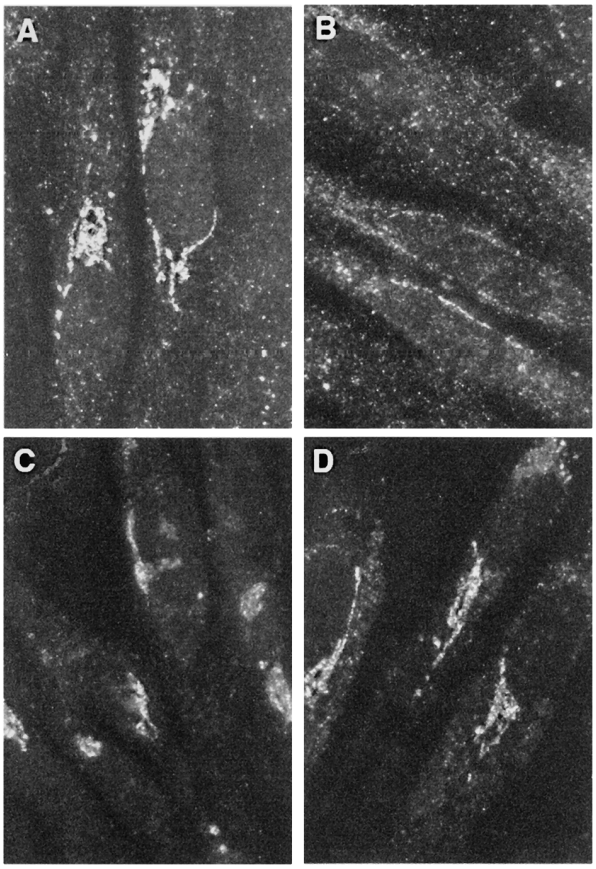

Fig. 1. U18666A prevents LDL-mediated release of OSBP from the Golgi apparatus. Human F8 fibroblasts were cultured on glass coverslips in MEM with 5% delipidated FCS for 3 days. Fibroblasts then received fresh MEM with 5% delipidated FCS with no addition (A), 50 μg human LDL/ml (B), 1 μg U18666A/ml (C), or 50 μg human LDL/ml plus 1 μg U18666A/ml (D). After 18 h, cells were processed for immunofluorescence localization of OSBP using antibody 104 and FITC-conjugated goat anti-rabbit secondary antibody as described in Materials and Methods.

The constitutive localization of OSBP in the Golgi apparatus in NPC and U18666A-treated cells could be due to trapping in a cholesterol-enriched compartment in the same manner that NPC1 protein is localized in cholesterol-enriched lysosomes in U18666A-treated cells (13). The possibility that a portion of OSBP co-localized with cholesterol was tested in control and NPC fibroblasts grown in the presence or absence of LDL by dual staining with filipin and an OSBP antibody (Fig. 3). Filipin staining in control F8 fibroblasts was weak and diffusely localized throughout the cell. The intensity of filipin fluorescence increased with LDL exposure but the localization was unaltered. OSBP was concentrated in the Golgi apparatus in F8 cells cultured in delipidated medium. In the two NPC cell lines (GM3123 and 93.41), there was intense staining of cholesterol in lysosomes in cells cultured with LDL. In both NPC fibroblasts cell lines, OSBP was concentrated in

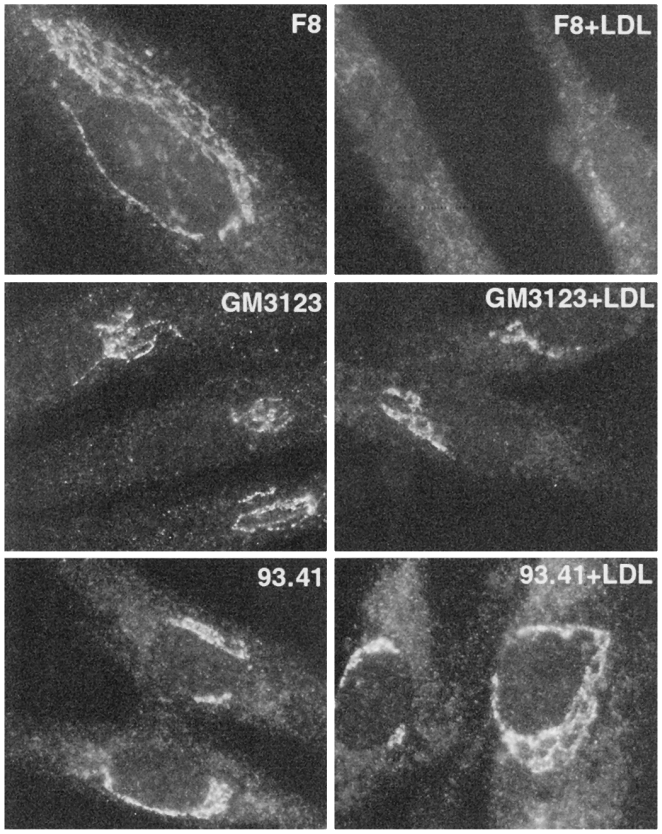

Fig. 2. Constitutive localization of OSBP in the Golgi apparatus in NPC fibroblasts. Control (F8) and NPC (GM3123 and 93.41) fibroblasts were cultured in MEM with 5% delipidated FCS for 3 days. Cells then received MEM with 5% delipidated FCS with or without human LDL (50 μg/ml). After 18 h, cells were processed for immunofluorescence localization of OSBP using antibody 104 and FITC-conjugated goat anti-rabbit secondary antibody as described in Materials and Methods.

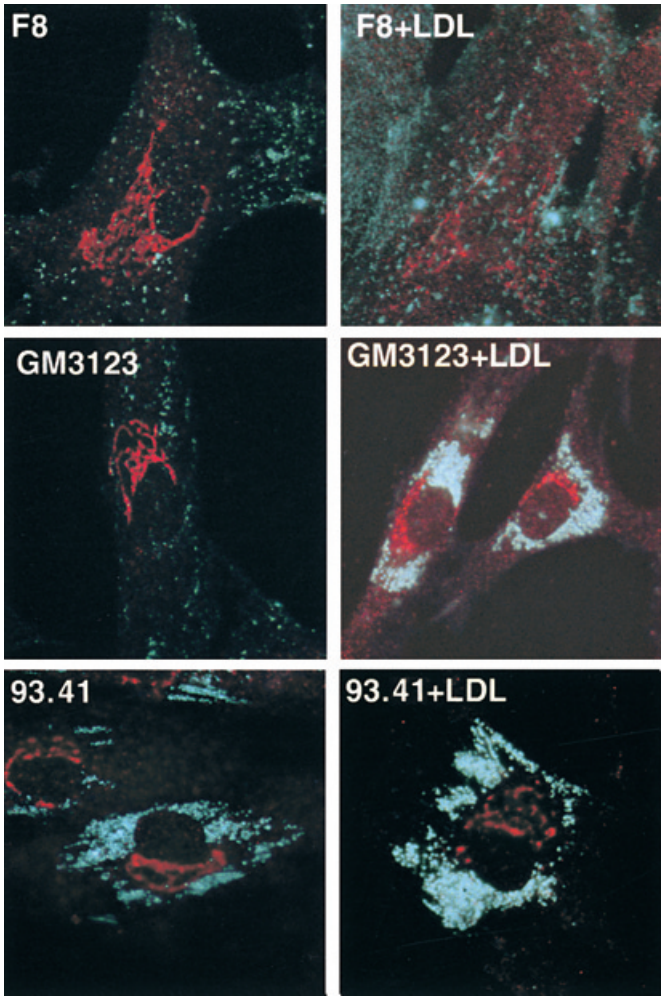

Fig. 3. OSBP does not co-localize with cholesterol in normal and NPC fibroblasts. Cells were cultured on glass coverslips in MEM with or without LDL (50 μg/ml), as described in the legend to Fig. 2. OSBP was localized in fixed and permeabilized cells with antibody 104 and a Texas Red-conjugated goat anti-rabbit secondary antibody. Cholesterol was localized by filipin staining. Images of Texas Red and filipin-stained cells were photographed and merged using Adobe Photoshop software.

a condensed Golgi region surrounded by cholesterol-engorged lysosomes. In the case of 93.41 fibroblasts, cholesterol was still evident in lysosomes of cells cultured in delipidated serum for 4 days. There was no apparent overlap of OSBP and filipin staining.

Results shown in Figs. 1–3 suggest that cholesterol efflux from lysosomes or endosomes mediated by NPC1 affected OSBP interaction with the Golgi apparatus. However, LDL, delipidated serum, or U18666A are also expected to influence de novo cholesterol synthesis in the ER, which could, in turn, affect OSBP localization. To determine whether endogenous synthesis was involved, cells were treated with combinations of LDL and lovastatin, a potent HMG-CoA reductase inhibitor that blocks cholesterol synthesis in the ER, and localization of OSBP was determined by indirect immunofluorescence (**Fig. 4**). When control fibroblasts were treated with medium containing delipidated serum or delipidated serum plus lovastatin (Fig. 4A and C, respectively), OSBP was strongly localized to the Golgi apparatus. Cells treated with LDL or LDL plus lovastatin (Fig. 4B and D, respectively) showed an identical pattern of diffuse staining and minimal Golgi localization, indicating that exogenous LDL-cholesterol was sufficient to induce OSBP translocation from the organelle.

OSBP expression in NPC and U18666A-treated cells

Immunoblot analysis of OSBP in NPC fibroblasts was performed to determine whether defective cholesterol transport altered OSBP expression or phosphorylation. An immunoblot of the total membrane fraction from control fibroblasts revealed a protein of approximately 170 kDa, corresponding to NPC1 (14). Both NPC fibroblast lines (GM3123 and 93.41) expressed greatly reduced levels of NPC1 protein (**Fig. 5A**). Total OSBP extracted from fibroblasts with Triton X-100 and detected by immunoblotting migrated as a doublet of 97–100 kDa (Fig. 5B), the high molecular mass form resulting from extensive phosphorylation of the protein on serine residues (29). The level of OSBP expression and the distribution between the two phosphorylated isoforms were similar in all the cell lines,

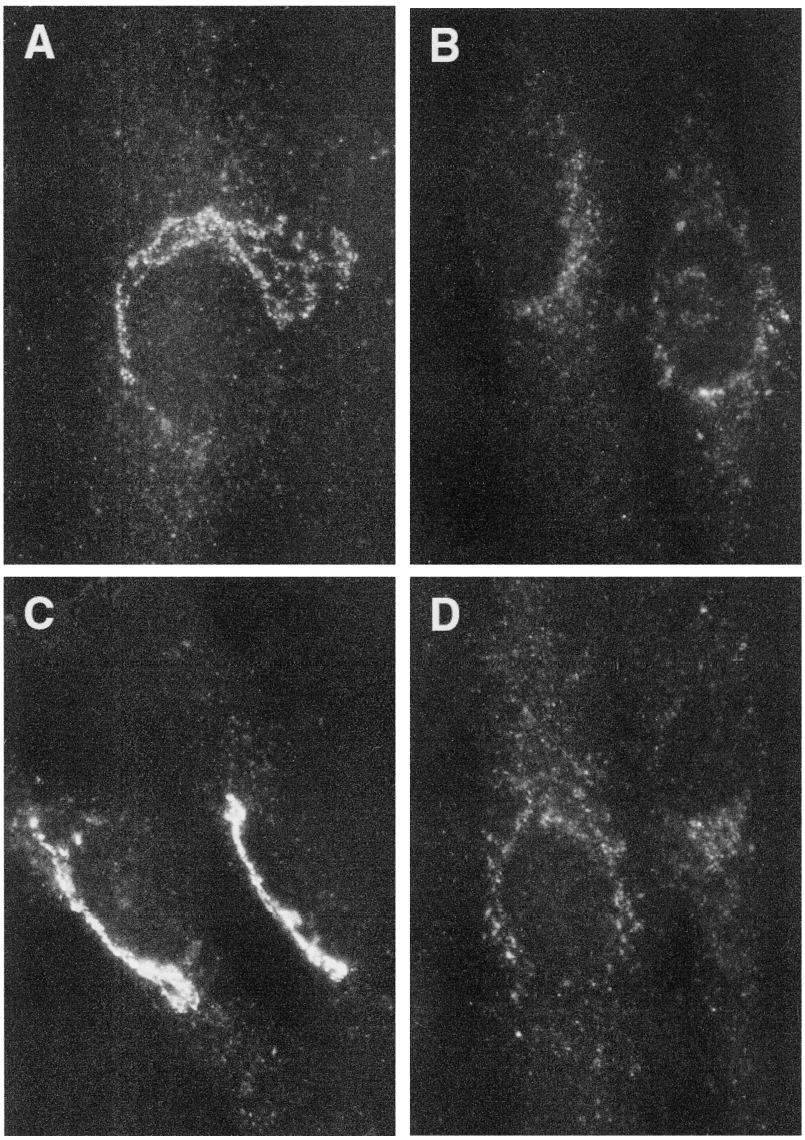

Fig. 4. Golgi localization of OSBP in response to inhibition of cholesterol synthesis by lovastatin is prevented by LDL. F8 fibroblasts were cultured in MEM with 5% delipidated FCS for 3 days. Cells then received fresh MEM with 5% delipidated FCS with no addition (A), 50 μg human LDL/ml (B), 5 μM lovastatin (C), or 5 μM lovastatin plus 50 μg human LDL/ml (D). After 12 h, cells were processed for immunofluorescence localization of OSBP as described in the legend to Fig. 1.

and were unaffected by growth in LDL. Similarly, there were no differences in OSBP expression or distribution in the particulate (membrane) and cytosolic fractions of NPC fibroblasts compared with controls (Fig. 5C).

U18666A treatment of cells mimicked the NPC phenotype in terms of constitutive OSBP localization to the Golgi apparatus (Figs. 1–3); however, there are biochemical differences between the genetic disorder and the drug-induced model. Most notable is the inhibition of cholesterol synthesis by U18666A at the step catalyzed by 2,3-oxidosqualene cyclase (30). This is in contrast to elevated and partially unregulated de novo cholesterol synthesis in NPC fibroblasts (27, 31). To confirm that U18666A inhibited cholesterol synthesis in our system, we treated fibroblasts and CHO cells with the drug (1 μg/ml) for up to 8 h, and analyzed the sterol profiles by [^{14}C]acetate labeling and TLC of labeled sterols. As expected, treatment with U18666A inhibited incorporation into cholesterol by >95% and caused the appearance of two nonpolar compounds corresponding in mobility to squalene 2,3-oxide and squalene 2,3:22,23-dioxide (results not shown). This confirms that U18666A is a potent inhibitor of both cholesterol synthesis and transport in CHO cells.

Previous observations that cholesterol depletion with lovastatin or in SRD 6 cells resulted in OSBP dephosphorylation (18) prompted us to test whether U18666A also altered OSBP phosphorylation because this drug blocks uptake and de novo synthesis of cholesterol. Previously, we showed that acute U18666A treatment for 1 h did not alter OSBP phosphorylation (17); therefore, the influence of the drug (1 μg/ml) was determined in NPC fibroblasts and CHO cells grown in the absence or presence of LDL for up to 24 h. The phosphorylation status of OSBP was determined by the relative amounts of the hypophosphorylated and hyperphosphorylated proteins that differ in relative mass by 2–3 kDa on SDS-PAGE (29). Initially, CHO cells were treated with increasing concentrations of U18666A for 4 h, and OSBP phosphorylation was assessed by immunoblotting (**Fig. 6A**). Compared with untreated CHO cells, U18666A caused a shift to the dephosphorylated low molecular mass form of OSBP. 25-Hydroxycho-

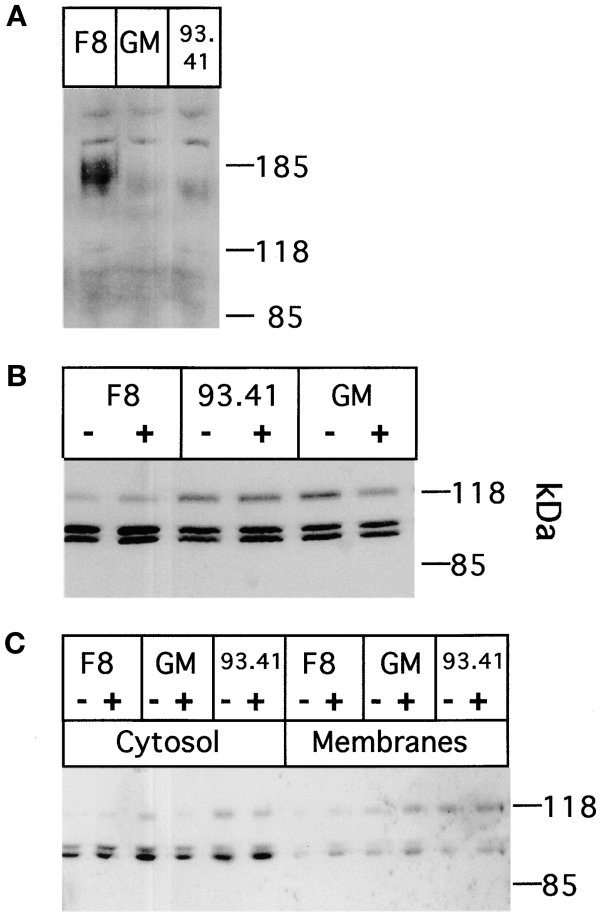

Fig. 5. Expression of OSBP in NPC fibroblasts. Fibroblasts were cultured in MEM with 5% delipidated FCS for 3 days prior to replacement with the same medium with (+) or without (−) LDL (50 μg/ml) for 18 h. The cytosolic and particulate fractions of cells were prepared and immunoblotted for NPC1 and OSBP as described in Materials and Methods. A: Total membrane fractions (25 μg protein) from control and NPC cells were resolved by SDS-6% PAGE, transferred to nitrocellulose, and analyzed by immunoblotting using the NPC1-C anti-peptide antibody. B: 0.3% Trition X-100 extracts (25 μg protein) of control and NPC fibroblasts treated with (+) or without (−) LDL were seperated by SDS-6% PAGE, transferred to nitocellulose, and immunoblotted for OSBP using antibody 170. C: OSBP expression in cytosolic and total membrane fractions (10 μg protein) from fibroblasts treated with (+) or without (−) LDL was determined using antibody 170.

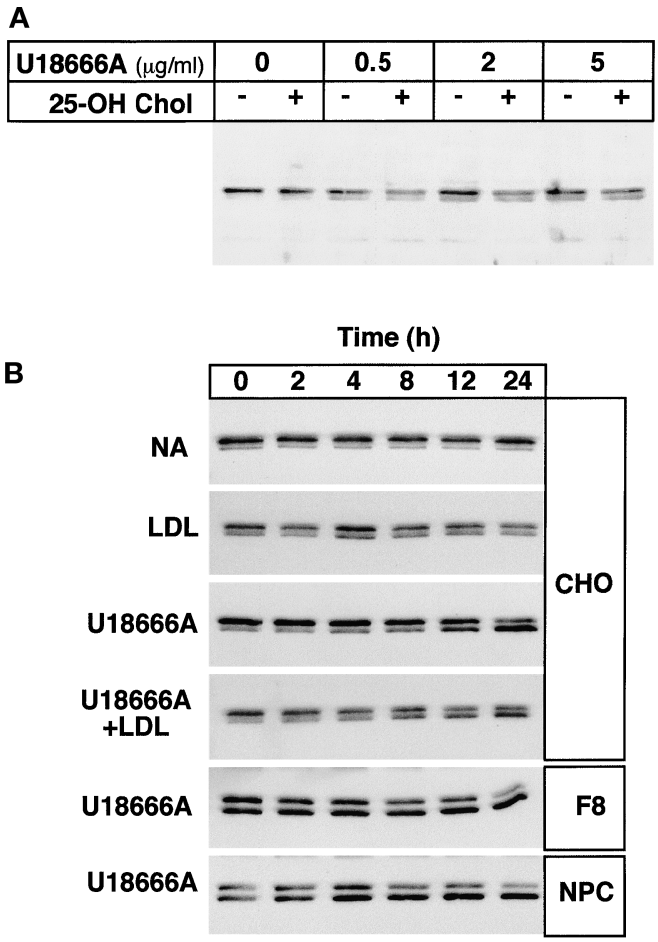

Fig. 6. Dephosphorylation of OSBP in U18666A-treated fibroblasts and CHO cells. A: CHO cells were cultured in DMEM with delipidated FCS for 24 h prior to the addition of the indicated concentration of U18666A with (+) or without (−) 2.5 μg 25-hydroxycholesterol (25-OH Chol)/ml for 4 h. OSBP in 0.5% Triton X-100 extracts was detected by immunoblotting with antibody 104. B: CHO cells were cultured in DMEM with 5% lipoprotein-deficient FCS for 6 h prior to the addition of 1 μg U18666A/ml, 1 μg U18666A/ml plus 50 μg LDL/ml, 50 μg LDL/ml, or no addition (NA). Untreated controls in each experiment (0 h) received solvent (DMSO or PBS) for 24 h. Fibroblasts were cultured in MEM with 5% delipidated FCS for 48 h prior to the addition of 1 μg U18666A/ml. At the indicated time points, Triton X-100 extracts of cells were prepared, resolved on SDS-6% PAGE, transferred to nitrocellulose, and immunoblotted with antibody 170 as described in Materials and Methods.

lesterol added to cells in the presence or absence of U18666A for 4 h did not alter phosphorylation of OSBP. Figure 6B shows the effects of U18666A on OSBP phosphorylation over a 24-h period. In CHO cells cultured in delipidated medium or LDL, OSBP was primarily in the high molecular mass hyperphosphorylated form, and there was no change in total expression and distribution between the two phosphorylated forms. CHO cells treated with U18666A or U18666A plus LDL displayed a progressive shift to the hypophosphorylated form of OSBP between 8 h and 12 h. By 24 h, the majority of OSBP was in the hypophosphorylated state. In normal and NPC fibroblasts (GM3123) treated with U18666A, OSBP dephosphorylation was first evident by 4 h or 8 h, and the protein was almost entirely in the hypophosphorylated form by 24 h. The treatments described in Fig. 6 did not affect cell morphology or viability (as assessed by trypan blue exclusion or yield of cell protein).

Localization of a cholesterol-sensitive phosphorylation site in OSBP

Results shown in Figs. 1 and 6 demonstrate that cholesterol depletion of cells cultured in delipidated medium with U18666A promotes dephosphorylation of OSBP in the Golgi apparatus. We sought to identify the cholesterol-sensitive phosphorylation site in OSBP that was responsible for the molecular mass shift. Initially, we analyzed the phosphorylation of C-terminal truncation mutants of

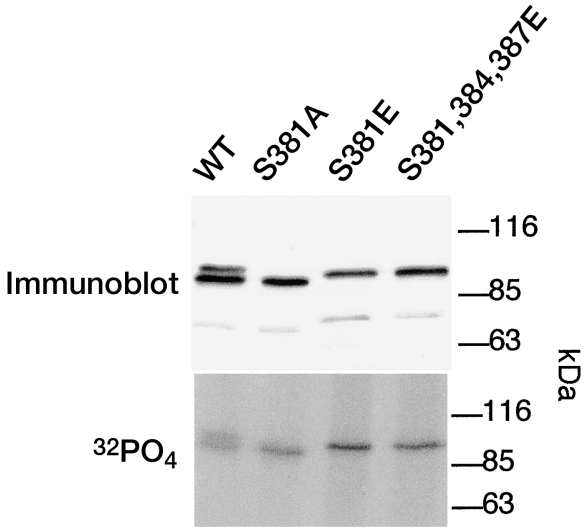

Fig. 7. Phosphorylation of serine 381 caused altered mobility of OSBP on SDS-PAGE observed during cholesterol depletion. Plasmids encoding wild-type OSBP and the indicated phosphorylation mutants were transiently transfected into CHO cells using Lipofectamine. Cells were harvested 48 h later in 0.5% Triton X-100 buffer and analyzed by immunoblotting (25 μg protein) using monoclonal antibody 11H9 (upper panel). A duplicate dish of cells was pulse-labeled with 25 μCi $^{32}PO_4$ /ml for 6 h. Cells were extracted in 0.5% Triton X-100, and OSBP was immunoprecipitated with 11H9 as described Materials and Methods (lower panel). Cell extracts or immunoprecipitates were resolved on SDS-6% PAGE. ^{32}P-OSBP in the lower panel was identified by autoradiography of the dried gel at −70°C for 3 days without an intensifying screen.

OSBP and tentatively identified a serine phosphorylation site between amino acids 280 and 400 that was responsible for the molecular mass shift (results not shown). Site-directed mutagenesis of candidate serine residues in this region to alanine identified this site as serine 381. To confirm that serine 381 of OSBP was phosphorylated in vivo and was responsible for the molecular mass shift on SDS-PAGE, cDNA encoding wild-type OSBP and OSBP S381A, OSBP S381E, and OSBP S381,384,387E were transiently transfected into CHO cells and analyzed by immunoblotting and $^{32}PO_4$ incorporation/immunoprecipitation. As expected, wild-type OSBP migrated as a closely spaced double on SDS-PAGE (**Fig. 7**, upper panel), and both bands incorporated $^{32}PO_4$ (lower panel). The S381A mutation caused a loss of the upper band, but the lower band still incorporated $^{32}PO_4$, indicating other phosphorylation sites in OSBP. If phosphorylation of serine 381 was responsible for the molecular mass shift, then substitution of a glutamic acid at this position should establish a permanent negative charge and decrease mobility on SDS-PAGE. Indeed, transiently transfected OSBP S381E co-migrated with the upper band of wild-type OSBP. We noted that there were two potential casein kinase I sites adjacent to serine 381, RTG**S**^{381}NI**S**^{384}GA**S**^{387}, that could be recognized following phosphorylation of serine 381 (32). Expression of OSBP with all three serines substituted for glutamic acids (S381,384,387E) did not cause a further shift in mass, and it did not appear to diminish $^{32}PO_4$ incorporation relative to OSBP S381A or OSBP S381E.

We analyzed the serine 381 phosphorylation site in more detail by in vivo $^{32}PO_4$-labeling, immunoprecipitation, and two-dimensional tryptic mapping of transiently transfected wild-type OSBP and three OSBP mutants with serine 381, 384, or 387 individually converted to alanine (**Fig. 8A**). The

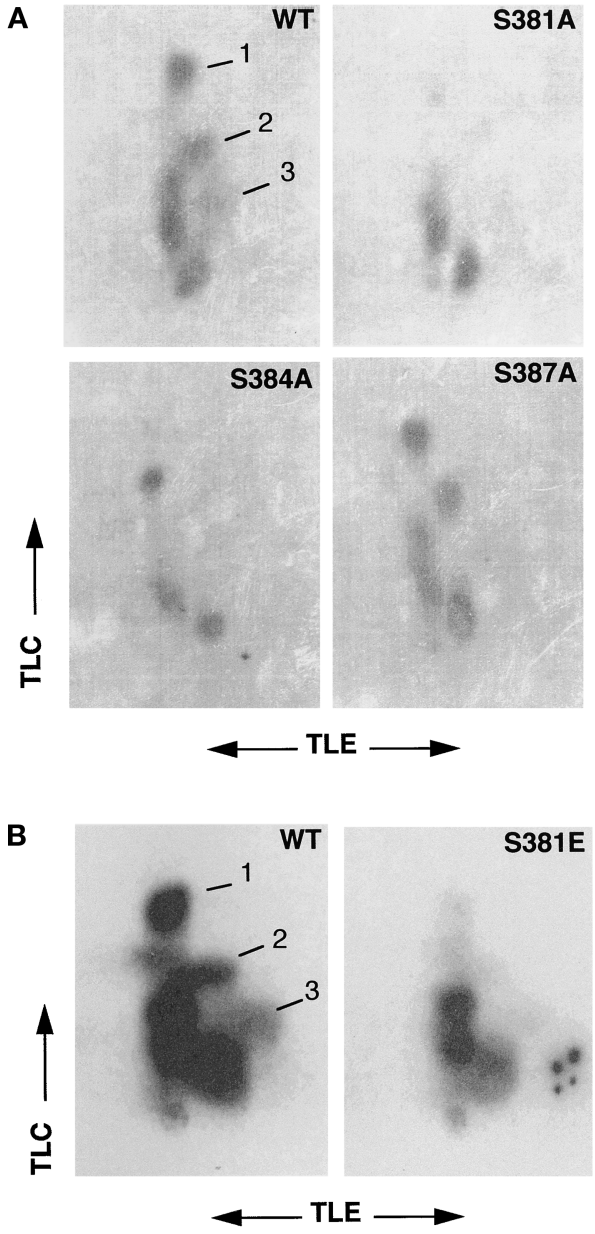

Fig. 8. Identification of phosphorylation sites on OSBP by tryptic phosphopeptide mapping. A*:* Plasmids encoding wild-type OSBP (WT), OSBP S381A, OSBP S384A, and OSBP S387A were transiently transfected into CHO cells using Lipofectamine. After 48 h, cells were labeled with 50 μCi $^{32}PO_4$/ml in 2 ml of DMEM with 5% dialyzed FCS for 6 h. Cells were harvested in 0.5% Triton X-100, ^{32}P-OSBP was immunoprecipitated with monoclonal 11H9, and subjected to tryptic mapping by two-dimensional thin-layer electrophoresis (TLE) and TLC as described in Materials and Methods. B*:* Wild-type OSBP (WT) and OSBP S381E were transfected into CHO cells and phosphopeptides analyzed as described above. The relevant phosphopeptides discussed in the text are numbered 1 to 3 in the wild-type OSBP panels. Autoradiograms are the result of exposure of the thin-layer plates to Kodak BioMax film for 3–5 days at −70°C.

tryptic map for in vivo labeled OSBP S381A revealed that this mutation removed three phosphopeptides compared with wild-type OSBP (numbers 1 to 3 in Fig. 8A). As mentioned above, phosphorylation at this site could promote subsequent phosphorylation of serines 384 and 387 by a casein kinase I-like activity (32). Indeed, tryptic maps of transiently transfected OSBP S384A and S387A revealed that each mutation removed a phosphopepetide from the tryptic map, with serine 387 being poorly phosphorylated relative to serine 381 and serine 384. Thus, phosphopeptides 1, 2, and 3 correspond to single, double, and triple phosphorylation on serines 381, 381–384, and 381–384–387, respectively. Figure 8B shows the tryptic phosphopeptide maps for wild-type and OSBP S381E. Although it was evident that conversion of serine 381 to a negatively charged amino acid was sufficient to cause a mobility shift on SDS-PAGE (see Fig. 7), a glutamic acid at this site was not sufficient to restore phosphorylation at serines 384 and 387.

DISCUSSION

Several pathways for sterol trafficking and regulation have been localized to the Golgi apparatus including raft/caveolae formation (15, 16, 21, 22), processing of SREBP (33), and regulation of LDL-cholesterol efflux from lysosomes (6). Using genetic and drug-induced models of altered cholesterol synthesis and transport, we demonstrated that OSBP is regulated by cholesterol at two levels. First, interaction of OSBP with elements of the Golgi apparatus occurred in response to changes in transport of LDL-derived cholesterol from lysosomes/endosomes. Second, OSBP phosphorylation at serine 381, 384, and 387 was regulated by cholesterol depletion due to cessation of LDL cholesterol transport and inhibition of de novo synthesis. These results implicate OSBP as an important downstream target for LDL cholesterol in the Golgi pathway.

The response of OSBP to changes in cholesterol homeostasis is summarized in the model shown in **Fig. 9**. This model illustrates three conditions of altered cholesterol balance in the cell: cholesterol supply via the LDL pathway (top panel), de novo synthesis of cholesterol in the ER (middle panel), and inhibition of the LDL receptor and de novo pathways (bottom panel). In control cells treated with LDL (Fig. 9, top panel), endogenous synthesis is suppressed, and the prominent route of cholesterol delivery is via the LDL receptor pathway. The majority of LDL cholesterol is transported from lysosomes or endosomes to the PM (7, 34), but a portion appears to bypass the PM and move directly to the ER (5, 6). Under these conditions, OSBP was diffusely localized in the cytoplasm or in small vesicles. Previously observed effects of LDL uptake on cholesterol distribution across the Golgi stacks (23, 24) and cholesterol delivery to the ER or PM via the Golgi could be the signal for OSBP dissociation to a cytoplasmic or vesicular pool. Cholesterol-regulated dissociation of OSBP from the Golgi was also seen in SRD 6 cells that do not synthesize cholesterol or express LDL receptors due to a defect in the site 2 protease that cleaves

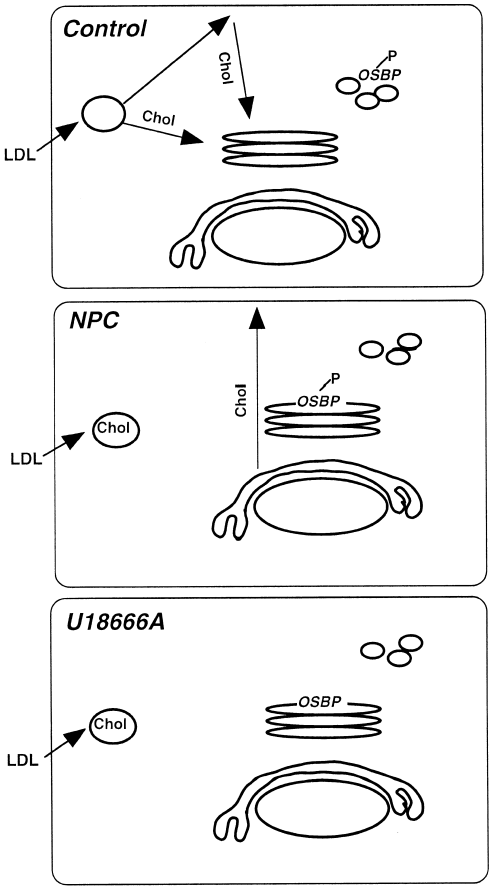

Fig. 9. A model for the regulation of OSBP phosphorylation and association with the Golgi apparatus by de novo synthesized and LDL-derived cholesterol.

SREBP (35). OSBP localized in the Golgi apparatus in cholesterol-starved SRD 6 cells dissociated to a cytoplasmic/vesicular pool when cells were incubated with cyclodextrin/cholesterol complexes (18). Presumably, cholesterol exchanged into cells in this manner was transported to the same site as LDL cholesterol, where it promoted OSBP release from the Golgi apparatus.

When cells were cultured in the absence of LDL or in NPC fibroblasts (Fig. 9, middle panel), OSBP associated with the Golgi apparatus. This suggests that cessation of cholesterol transport from a lysosomal/endosomal compartment generates a signal, perhaps related to altered Golgi cholesterol content, that triggers OSBP translocation to the Golgi apparatus. Another possibility is that OSBP translocates in response to increased ER synthesis of cholesterol. However, two observations suggest that this is unlikely. First, OSBP was intensely localized to the Golgi when fibroblasts were treated with lovastatin, a condition that was reversed by addition of LDL (Fig. 4). Second, OSBP was also localized to the Golgi apparatus in SRD 6 cells that have cholesterol synthetic rates of 5% of controls (36). This suggests that cholesterol synthesis in the ER does not greatly influence translocation of OSBP to the Golgi apparatus. Cyclodextrin treatment of CHO cells grown in

LDL also caused intense Golgi localization of OSBP (17). This result can now be interpreted on the basis of a recent report that LDL cholesterol exits the lysosomes or endosomes in CHO cells and first appears in a PM pool that is accessible to cyclodextrins (7). This suggests that cyclodextrin promoted OSBP localization to the Golgi by removing LDL-derived cholesterol from the PM and preventing its subsequent internalization. This further supports a model where OSBP localizes to the Golgi apparatus in response to cholesterol depletion, and that de novo synthesis is either insufficient to supply enough cholesterol to reverse this process or is transported through a compartment or by a mechanism not involving OSBP.

In the final condition, cells were starved for cholesterol by the combined inhibition of the LDL receptor pathway and de novo synthesis by U18666A (Fig. 9, lower panel). The resulting sterol depletion caused extensive dephosphorylation of OSBP. Previous results showing OSBP dephosphorylation in cholesterol auxotrophic SRD 6 cells and lovastatin-treated CHO cells cultured in delipidated serum (18) supports our conclusion that dephosphorylation is a specific response to sterol depletion, and occurs after OSBP is localized to the Golgi apparatus.

Initially, OSBP was shown to translocate to the Golgi apparatus in CHO cells in response to addition of exogenous oxysterol such as 25-hydroxycholesterol (19, 20). Translocation is mediated by the pleckstrin homology domain of OSBP (19, 37) through interactions with phosphatidylinositol polyphosphates (37, 38), and is negatively regulated by the C-terminal ligand binding domain (20). An explanation of OSBP translocation that involves oxysterol binding could explain the various responses shown in Fig. 9. Because this model predicts that OSBP is localized to the Golgi apparatus when cells are actively synthesizing cholesterol in the ER, but not when the pathway is suppressed by LDL, it is feasible that an oxysterol intermediate of the biosynthetic pathway is produced that binds OSBP and promotes translocation. However, this explanation is not supported by our finding that OSBP is also strongly localized to the Golgi apparatus under conditions where de novo synthesis is inhibited [(18, 17), this study] and oxysterol synthesis should be greatly reduced. This implies that OSBP localization to the Golgi is not in response to oxysterols, but due to another signal or ligand generated as a consequence of sterol depletion. Because cholesterol depletion also promotes OSBP dephosphorylation, we cannot rule out the possibility that this effect enhances the association of OSBP with the Golgi apparatus. This is not likely due to a direct effect on ligand binding because hypo- and hyperphosphorylated forms of OSBP, produced by treatment with staurosporine and okadaic acid, respectively, had similar in vitro [^{3}H]25-hydroxycholesterol binding activity (29).

The involvement of phosphorylation in localization of OSBP to the Golgi apparatus can now be more accurately defined with the identification of a sterol-sensitive phosphorylation site responsible for the reduced mobility on SDS-PAGE observed in U18666A-treated cells. The sequence around this site, RTG**S**^{381}NI**S**^{384}GA**S**^{387}, predicts that serine 381 is phosphorylated by a kinase that recognizes a basic residue at the +3 position such as protein kinase A (PKA), protein kinase C (PKC), or S6 kinase. However, of the numerous PKC, PKA, and other protein kinase inhibitors tested for effects on OSBP phosphorylation, only staurosporine altered mobility on SDS-PAGE or $^{32}PO_4$ incorporation [(29) and unpublished results]. Another feature of this site is its requirement for subsequent phosphorylation at serines 384 and 387. This is a classic recognition motif for casein kinase I, which requires prior phosphorylation of a +3 serine or threonine (32). This is the case with OSBP because conversion of serine 381 to alanine blocked phosphorylation of serines 384 and 387 (Fig. 8). Conversion of serine 381 to glutamic acid to generate a constitutive negative charge restored the mass shift on SDS-PAGE (Fig. 7), but did not promote phosphorylation of serines 384 or 387, suggesting the kinase that phosphorylates serines 384 and 387 absolutely requires a phosphoserine at position 381. The current data do not allow us to identify how sterols influence phosphorylation at serine 381, which could involve direct or indirect regulation of kinases or phosphatases. Dephosphorylation of OSBP occurs in the Golgi apparatus, based on inhibition of phosphorylation at serines 381, 384, and 387 by brefeldin A, as assessed by tryptic phosphopeptide maps and altered mobility on SDS-PAGE (29).

Our studies with NPC1 fibroblasts and U18666A have identified OSBP as a potential early downstream target for the NPC1 protein. OSBP did not co-localize with lysosomal cholesterol or lysosomal markers such as LAMP 1 (results not shown) in control or NPC fibroblasts. Results from fibroblasts and transfected CHO cells have shown that NPC1 is localized to a lysosomal or late endosomal compartment (13). This suggests that NPC1 and OSBP do not co-localize, and NPC1 affects OSBP localization primarily by releasing cholesterol from its compartment and not via a direct interaction. Defective release of OSBP from the Golgi apparatus in response to attenuated transport of cholesterol from lysosomes in NPC fibroblasts is similar, in many respects, to effects of the NPC1 mutation on other aspects of cholesterol homeostasis. Thus, diminished ACAT activation and delayed cholesterol regulatory responses (27, 39) in NPC cells indicates that cholesterol is not reaching the ER, whereas constitutive Golgi localization of OSBP suggests a paucity of sterol in that organelle.

This work was supported by a Canadian Institutes of Health Research Group Grant and Scientist Award (N.D.R). We thank Robert Zwicker and Gladys Keddy for assistance with cell culture. The NPC1-C antibody and 93.41 and 98.16 NPC fibroblasts were kindly provided by Peter Penchev and Joan Blanchette-Mackie (National Institutes of Health, Bethesda, MD).

Manuscript received 25 January 2001 and in revised form 5 March 2001.

REFERENCES

1. Brown, M. S., and J. L. Goldstein. 1990. Regulation of the mevalonate pathway. *Nature.* **343:** 425–430.
2. Liscum, L., and N. J. Munn. 1999. Intracellular cholesterol transport. *Biochim. Biophys. Acta.* **1438:** 19–37.
3. Lange, Y., and T. L. Steck. 1997. Quantitation of the pool of choles-

terol associated with acyl-CoA:cholesterol acyltransferase in human fibroblasts. *J. Biol. Chem.* **272:** 13103–13108.
4. Lange, Y., M. H. Swaisgood, B. V. Ramos, and T. L. Steck. 1989. Plasma membrane contains half the phospholipid and 90% of the cholesterol and sphingomyelin in cultured fibroblasts. *J. Biol. Chem.* **264:** 3786–3793.
5. Underwood, K. W., N. L. Jacobs, A. Howley, and L. Liscum. 1998. Evidence for a cholesterol transport pathway from lysosomes to endoplasmic reticulum that is independent of the plasma membrane. *J. Biol. Chem.* **273:** 4266–4274.
6. Neufeld, E. B., A. M. Cooney, J. Pitha, A. E. Dawidowicz, N. K. Dwyer, P. G. Pentchev, and E. J. Blanchette-Mackie. 1996. Intracellular trafficking of cholesterol monitored with cyclodextrins. *J. Biol. Chem.* **271:** 21604–21613.
7. Cruz, J. C., S. Sugii, C. Yu, and T-Y. Chang. 2000. Role of Niemann-Pick Type C1 protein in intracellular trafficking of low density lipoprotein-derived cholesterol. *J. Biol. Chem.* **275:** 4013–4021.
8. Kaplan, M. R., and R. D. Simoni. 1985. Transport of cholesterol form the endoplasmic reticulum to the plasma membrane. *J. Cell. Biol.* **101:** 446–453.
9. Slotte, J. P., and E. L. Biermann. 1988. Depletion of plasma membrane sphingomyelin rapidly alters the distribution of cholesterol between plasma membrane and intracellular pools in cultured fibroblasts. *Biochem. J.* **250:** 653–658.
10. Ridgway, N. D. 2000. Interactions between metabolism and intracellular distribution of cholesterol and sphingomyelin. *Biochim. Biophys. Acta.* **1484:** 129–141.
11. Hua, X., A. Nohturff, J. L. Goldstein, and M. S. Brown. 1996. Sterol resistance in CHO cells traced to a point mutation in SREBP cleavage activating protein. *Cell.* **87:** 415–426.
12. Carstea, E. D., J. A. Morris, K. G. Coleman, S. K. Loftus, D. Zhang, C. Cummings, J. Gu, M. A. Rosenfeld, W. J. Paven, D. B. Krizman, J. Nagle, M. H. Polymeropoulos, S. L. Sturley, Y. A. Ioannou, M. E. Higgins, M. Comly, A. Cooney, A. Brown, C. R. Kaneski, E. J. Blanchettee-Mackie, N. K. Dwyer, E. B. Neufeld, T-Y. Chang, L. Liscum, J. F. Strauss III, K. Ohno, M. Zeigler, R. Carmi, J. Sokol, D. Markie, R. R. O'Neill, O. P. van Diggelen, M. Elleder, M. C. Patterson, R. O. Brady, M. T. Vanier, P. G. Pentchev, and D. A. Tagle. 1997. Niemann-Pick C1 disease gene: homology to mediators of cholesterol homeostasis. *Science.* **277:** 228–231.
13. Neufeld, E. B., M. Wastney, S. Patel, S. Suresh, A. M. Cooney, N. K. Dwyer, C. F. Roff, K. Ohno, J. A. Morris, E. D. Carstea, J. P. Incardona, J. F. Strauss III, M. T. Vanier, M. C. Paterson, R. O. Brady, P. G. Pentchev, and E. J. Blanchette-Mackie. 1999. The Niemann-Pick C1 protein resides in a vesicular compartment linked to retrograde transport of multiple lysosomal cargo. *J. Biol. Chem.* **274:** 9627–9635.
14. Watari, H., E. J. Blanchette-Mackie, N. K. Dwyer, M. Watari, E. B. Neufeld, S. Patel, P. G. Pentchev, and J. F. Strauss III. 1999. Mutations in the leucine zipper motif and sterol sensing domain inactivate the Niemann-Pick C1 protein. *J. Biol. Chem.* **274:** 21861–21866.
15. Smart, E. J., Y. Ying, W. C. Donzell, and R. G. W. Anderson. 1996. A role for caveolin in transport of cholesterol from endoplasmic reticulum to plasma membrane. *J. Biol. Chem.* **271:** 29427–29435.
16. Smart, E. J., Y. Ying, P. A. Conrad, and R. G. W. Anderson. 1994. Caveolin moves from the caveolae to the Golgi apparatus in response to cholesterol oxidation. *J. Cell Biol.* **127:** 1185–1197.
17. Ridgway, N. D., T. A. Lagace, H. W. Cook, and D. M. Byers. 1998. Differential effects of sphingomyelin hydrolysis and cholesterol transport on oxysterol binding protein phosphorylation and Golgi localization. *J. Biol. Chem.* **273:** 31621–31628.
18. Storey, M. K., D. M. Byers, H. W. Cook, and N. D. Ridgway. 1998. Cholesterol regulates oxysterol binding protein phosphorylation and Golgi localization in Chinese hamster ovary cells: correlation with stimulation of sphingomyelin synthesis. *Biochem. J.* **336:** 247–257.
19. Lagace, T. A., D. M. Byers, H. W. Cook, and N. D. Ridgway. 1997. Abnormal cholesterol and cholesterol ester synthesis in Chinese hamster ovary cells overexpressing the oxysterol binding protein is dependent on the pleckstrin homology domain. *Biochem. J.* **326:** 205–213.
20. Ridgway, N. D., P. A. Dawson, Y. K. Ho, M. S. Brown, and J. L. Goldstein. 1992. Translocation of oxysterol binding protein to the Golgi apparatus triggered by ligand binding. *J. Cell Biol.* **116:** 307–319.
21. Anderson, R. G. 1998. The caveolae membrane system. *Annu. Rev. Biochem.* **67:** 199–225.
22. Heino, S., S. Lusa, P. Somerharju, C. Ehnholm, V. M. Olkkonen, and E. Ikonen. 2000. Dissecting the role of the Golgi complex and lipid rafts in biosynthetic transport to the cell surface. *Proc. Natl. Acad. Sci. USA.* **97:** 8375–8380.
23. Orci, L., R. Montesano, P. Meda, F. Malaisse-Lagae, D. Brown, A. Perrelet, and P. Vassalli. 1981. Heterogenous distribution of filipin-cholesterol complexes across the cisternae of the Golgi apparatus. *Proc. Natl. Acad. Sci. USA* **78:** 293–297.
24. Coxey, R. A., P. G. Pentchev, G. Campell, and E. J. Blanchette-Mackie. 1993. Differential accumulation of cholesterol in Golgi compartments of normal and Niemann-Pick type C fibroblasts incubated with LDL: a cytochemical freeze-fracture study. *J. Lipid Res.* **34:** 1165–1176.
25. Keller, P., and K. Simons. 1998. Cholesterol is required for surface transport of influenza virus hemagluttinin. *J. Cell Biol.* **140:** 1357–1367.
26. Hansen, G. H., L-L. Niels-Christiansen, E. Thorsen, L. Immerdal, and E. M. Danielsen. 2000. Cholesterol depletion in enterocytes: effect of the Golgi complex and apical membrane trafficking. *J. Biol. Chem.* **275:** 5136–5142.
27. Liscum, L., and J. R. Faust. 1987. LDL-mediated suppression of cholesterol synthesis and LDL uptake is defective in Niemann-Pick type C fibroblasts. *J. Biol. Chem.* **262:** 17002–17008.
28. Goldstein, J. L., S. K. Basu, and M. S. Brown. 1983. Receptor-mediated endocytosis of LDL in cultured cells. *Methods Enzymol.* **98:** 241–260.
29. Ridgway, N. D., K. Badiani, D. M. Byers, and H. W. Cook. 1997. Inhibition of phosphorylation of the oxysterol binding protein by brefeldin A. *Biochim. Biophys. Acta.* **1390:** 37–51.
30. Sexton, R. C., S. R. F. Panini Azran, and H. Rudney. 1983. Effects of 3β-[2-(diethylamino)ethoxy]androst-5-en-17-one on the synthesis of cholesterol and ubiquinone in rat intestinal epithelial cell cultures. *Biochemistry.* **22:** 5687–5692.
31. Ory, D. S. 2000. Niemann-Pick C: a disorder of cellular cholesterol trafficking. *Biochim. Biophys. Acta.* **1529:** 331–339.
32. Gross, S. D., and R. A. Anderson. 1998. Casein kinase I: spatial organization and positioning of a multifunctional protein kinase family. *Cell. Signal.* **10:** 699–711.
33. Nohturfft, A., D. Yabe, J. L. Goldstein, M. S. Brown, and P. J. Espenshade. 2000. Regulated step in cholesterol feedback localized to budding of SCAP from ER membranes. *Cell.* **102:** 315–323.
34. Lang, Y., J. Ye, and J. Chin. 1997. The fate of cholesterol exiting lysosomes. *J. Biol. Chem.* **272:** 17018–17022.
35. Sakai, J., E. A. Duncan, R. B. Rawson, X. Hua, M. S. Brown, and J. L. Goldstein. 1996. Sterol-regulated release of SREBP-2 from cell membranes requires two sequential cleavages, one within a transmembrane domain. *Cell.* **85:** 1037–1046.
36. Evans, M. J., and J. E. Metherall. 1993. Loss of transcriptional activation of three sterol-regulated genes in mutant hamster cells. *Mol. Cell. Biol.* **13:** 5175–5185.
37. Levine, T. P., and S. Munro. 1998. The pleckstrin homology domain of oxysterol binding protein recognizes a determinant specific to Golgi membranes. *Curr. Biol.* **8:** 729–739.
38. Rameh, L. E., A. Arvidsson, K. L. Carraway III, A. D. Couvillon, G. Aathbun, A. Crompton, B. VanRenterghem, M. P. Czech, K. S. Ravichandran, S. J. Burakoff, D-S. Wang, C-S. Chen, and L. C. Cantley. 1997. A comparative analysis of the phosphoinositide binding specificity of pleckstrin homology domains. *J. Biol. Chem.* **272:** 22059–22066.
39. Byers, D. M., J. Douglas, H. W. Cook, F. B. Palmer, N. D. Ridgway. 1994. Regulation of intracellular cholesterol metabolism is defective in lymphoblasts form Niemann-Pick type C and D patients. *Biochim. Biophys. Acta* **1226:** 173–180.